HHS Public Access

Author manuscript

Health Phys. Author manuscript; available in PMC 2017 November 27.

Published in final edited form as:

Health Phys. 2016 June ; 110(6): 612–622. doi:10.1097/HP.0000000000000496.

USE OF TRANSPORTABLE RADIATION DETECTION INSTRUMENTS TO ASSESS INTERNAL CONTAMINATION FROM INTAKES OF RADIONUCLIDES PART I: FIELD TESTS AND MONTE CARLO SIMULATIONS

Robert Anigstein[*], **Michael C. Erdman**[†], and **Armin Ansari**[‡]

[*]S. Cohen & Associates, 1608 Spring Hill Road, Vienna, VA 2218

[†]Department of Radiology, Milton S. Hershey Medical Center, Hershey, PA 17033-2390

[‡]Radiation Studies Branch, EHHE, NCEH, Centers for Disease Control and Prevention, Atlanta, GA 30341-3717

Abstract

The detonation of a radiological dispersion device or other radiological incidents could result in the dispersion of radioactive materials and intakes of radionuclides by affected individuals. Transportable radiation monitoring instruments could be used to measure photon radiation from radionuclides in the body for triaging individuals and assigning priorities to their bioassay samples for further assessments. Computer simulations and experimental measurements are required for these instruments to be used for assessing intakes of radionuclides. Count rates from calibrated sources of ^{60}Co, ^{137}Cs, and ^{241}Am were measured on three instruments: a survey meter containing a 2.54 × 2.54-cm NaI(Tl) crystal, a thyroid probe using a 5.08 × 5.08-cm NaI(Tl) crystal, and a portal monitor incorporating two 3.81 × 7.62 × 182.9-cm polyvinyltoluene plastic scintillators. Computer models of the instruments and of the calibration sources were constructed, using engineering drawings and other data provided by the manufacturers. Count rates on the instruments were simulated using the Monte Carlo radiation transport code MCNPX. The computer simulations were within 16% of the measured count rates for all 20 measurements without using empirical radionuclide-dependent scaling factors, as reported by others. The weighted root-mean-square deviations (differences between measured and simulated count rates, added in quadrature and weighted by the variance of the difference) were 10.9% for the survey meter, 4.2% for the thyroid probe, and 0.9% for the portal monitor. These results validate earlier MCNPX models of these instruments that were used to develop calibration factors that enable these instruments to be used for assessing intakes and committed doses from several gamma-emitting radionuclides.

Keywords

counting efficiency; Monte Carlo; detector; scintillation; whole-body counting

For correspondence contact: Robert Anigstein, PhD, S. Cohen & Associates, 740 West End Avenue, Apt. 95A, New York, NY 10025, or at anigstein@cs.com.

The authors declare no conflicts of interest.

INTRODUCTION

A radiological emergency, such as the detonation of a radiological dispersion device (RDD or “dirty bomb”), a severe reactor accident, or the surreptitious introduction of radioactive materials into food or drinking water could result in a large number of people being internally contaminated. There would be a need to screen these individuals rapidly for internal contamination to help determine if medical intervention is warranted. Such screening could also provide reassurance to potentially contaminated individuals who do not, in fact, have significant levels of internal contamination, and to their families.

Intakes of radionuclides can be assessed by in vitro bio-assay (e.g., urinalysis) or by use of radiation detection instruments that measure radiation emitted by radionuclides in the body (direct or in vivo bioassay). The latter method, which customarily employs whole body counters, can yield immediate estimates of intakes and doses from radionuclides that emit energetic photons or beta rays that produce bremsstrahlung x rays. However, due to their limited availability, existing whole body counters may not be adequate for screening large numbers of potentially affected individuals.

On the other hand, portable or transportable radiation monitoring instruments are widely available and can be used to rapidly screen individuals for beta- or gamma-emitting radionuclides. Such triage can assist in assigning priorities to affected individuals or to their urine samples for more definitive laboratory assessment. While many of these instruments can measure the radiation emitted from the human body following intakes of certain radionuclides, computer simulations that are validated by experimental measurements are needed for the instruments to provide reliable estimates of intakes and committed internal doses.

Previous studies

Several previous studies have aimed to develop computer models of radiation detection instruments that could be deployed in the field to assess internal contamination of individuals following intakes of radionuclides.

Kramer et al. (2005) used a high-purity germanium detector coupled to a multichannel analyzer (MCA) to measure count rates from discrete radioactive sources embedded in plastic disks, as well as from volume sources consisting of aqueous solutions of radionuclides contained in hollow compartments of anthropomorphic phantoms. The authors then constructed a model of the detector using the MCNP5 (Monte Carlo N-Particle, Version 5) radiation transport computer code and used the model to simulate the measured count rates. The results showed an average ratio of 1.39:1 of the MCNP[§] simulations of the discrete sources to the experimental measurements, over an energy range of 60–1,173 keV. The authors attributed the differences between the measured and calculated count rates to the

[§]The term “MCNP” refers to a family of codes that includes MCNP5, MCNPX, and MCNP6. In the present paper, the term “MCNP5” or “MCNPX” is used to refer to the use of that specific code and to features that are unique to that code; the generic term “MCNP” is used to describe features and capabilities common to the MCNP family.

limited information on the detector obtainable from the manufacturer (due to the constraints of its proprietary design) that prevented the construction of a more accurate MCNP model.

Scarboro et al. (2009) used MCNP5 to construct a model of the Captus 3000 thyroid uptake probe (Capintec Inc., Sales and Marketing and Customer Support, Ramsey, NJ, USA). The authors then used the model to simulate the count rates from each of six discrete radioactive sources placed inside a polymethyl methacrylate (PMMA) slab phantom, with various thicknesses of PMMA between the source and the detector. Results were reported for three radionuclides: ^{22}Na, ^{137}Cs, and ^{241}Am. For ^{22}Na, the ratio of MCNP simulations to experimental results over a range of 0–108 mm of PMMA varied from 0.96 to 0.99 with an average of 0.97. Corresponding results for ^{137}Cs showed a range of 0.90–0.95 with an average of 0.93, while for ^{241}Am, the ratios ranged from 1.18 to 1.36 with an average of 1.31. Thus, while the agreement was excellent for ^{22}Na, the highest-energy gamma emitter, the agreement declined for the two radio-nuclides with lower-energy emissions.

Manger et al. (2012) used the same slab phantom and radioactive sources and a methodology similar to that of Scarboro et al. (2009) to construct and test MCNP models of two plastic scintillation detectors: the Canberra Syrena Handheld Search Monitor (no information on current availability) and the Thermo Micro Rem Tissue Equivalent Survey Meter (current version: Thermo Micro Rem/Sievert Tissue-Equivalent Survey Meter; available from Thermo Fisher Scientific Inc., Waltham, MA, USA). Because the measured count rates were significantly lower than the MCNP5 simulations, the authors developed scaling factors for each radionuclide-detector combination, ranging from 0.15 for ^{241}Am measured with the Syrena monitor to 0.82 for ^{137}Cs and the Micro Rem meter. These factors were to be used to adjust the modeled counts from an individual internally contaminated with one of these radionuclides to yield the expected count rate on the corresponding instrument. The authors suggested that the differences between the measured and simulated counts may have been due to differences in material compositions and densities between the physical detectors and the MCNP models.

Dewji et al. (2013) constructed and tested an MCNP5 model of the Canberra Model 802 Scintillation Detector (Canberra Industries Inc., Meriden, CT, USA), which incorporates a 5.08 × 5.08-cm NaI(Tl) crystal. The authors used the same radioactive sources and slab phantom as Scarboro et al. (2009). However, instead of accumulating gross counts, they connected the detector to an MCA and used the system to collect counts in 1,024 energy bins with a dispersion of 3.17 keV per channel. They used their MCNP model to simulate the counts in the same energy bins, employing the MCNP Gaussian energy-broadening (GEB) option, described later in the present paper, to simulate the statistical broadening of the photopeaks. They then compared the count rates in the photopeak regions of each radionuclide in the experimental and simulated spectra. These regions were selected manually to encompass the counts in each photopeak, or in groups of photopeaks, for radionuclides with several closely spaced gamma-ray emissions in the experimental and simulated spectra. The authors applied scaling factors to account for differences in the count rates in individual photopeak regions of the six radionuclides used in the study. These scaling factors ranged from 0.85 for the high-energy (1,173.2 and 1,332.5 keV) gamma rays from ^{60}Co to 1.0 (i.e., no correction) for the 59.5-keV gamma ray of ^{241}Am.

Present work

Anigstein et al. (2007–2010) demonstrated that radiation detection and imaging systems commonly found in hospitals could be used to screen individuals for radionuclides taken into the body. The current study extends these investigations to three transportable instruments—the Ludlum Model 44-2 sodium iodide (NaI[Tl]) gamma scintillator (Ludlum Measurements Inc., Sweetwater, TX, USA), the Captus 3000 thyroid uptake probe, and the Transportable Portal Monitor Model TPM-903B (Rapiscan Systems, Longmont, CO, USA)—that could potentially be used for such screening after a radiological incident. One objective of the present study was to accurately model the response of these instruments in order to obtain good agreement with actual measurements without the use of empirical radionuclide-dependent scaling factors, such as those employed by other investigators.

The first step was the measurement of count rates from discrete radioactive sources of ^{60}Co, ^{137}Cs, and ^{241}Am to validate the computer models that had been constructed of these instruments using the Monte Carlo radiation transport code MCNPX 2.7.0 (Monte Carlo N-Particle eXtended; LANL 2011). The radionuclides were selected from the “nine isotopes of interest for RDDs” listed by ANL (2007). Americium-241 was included in these experiments to provide validation for low-energy photons—its principal gamma ray has an energy of 59.54 keV. Because of the low efficiency of these instruments for detecting this nuclide, combined with its high dose coefficients, they would most likely not be effective for screening individuals for intakes of this radionuclide below the Clinical Decision Guide of 250 mSv for adult men and nonpregnant adult women (NCRP 2008).

The measurements were performed at the Penn State Milton S. Hershey Medical Center in Hershey, PA.

MATERIALS AND METHODS

Radioactive calibration sources

Radioactive calibration sources used in the experiment comprised ^{60}Co and ^{137}Cs [Catalog Nos. GF-060-D and GF-137-D, Isotope Products Laboratories (now Eckert & Ziegler Isotope Products Inc.), Valencia, CA, USA], and ^{241}Am (Model CAL2600 Gamma Standard, North American Scientific, Inc., Chatsworth, CA, USA).** All three sources are traceable to the National Institute of Standards and Technology. Each ^{60}Co and ^{137}Cs source consists of evaporated salts that had been deposited at the bottom of a cylindrical cavity in an acrylic disk, after which the cavity had been plugged with an epoxy resin. The source was modeled as a circular area, 5 mm in diameter and 2.77 mm from the face of the acrylic disk. The ^{241}Am source is in the form of a resin bead, 1 mm in diameter, mounted in the center of a 3-mm-thick acrylic disk, and was modeled as a point source.†† Table 1 lists the activity of each source based on the activity certified by the manufacturer, corrected for radioactive decay using the half-lives listed in the table. Both manufacturers cited uncertainties at the

**Since the ^{241}Am source was procured, the calibration source business of North American Scientific Inc. was acquired by Eckert & Ziegler Isotope Products Inc.

††Simulations of the ^{241}Am source distributed over the spherical volume produced count rates that were the same as those from a point source, within the uncertainties due to Monte Carlo statistics. The simpler point-source model was used in the interest of computational efficiency.

99% confidence levels. The coefficient of variation (c_v) of the activity of each source was derived from its cited uncertainty, assuming the uncertainties were normally distributed. In performing the experimental measurements, the edge of each source disk was attached to the end of a 1.27-cm-diameter acrylic rod in order to minimize photon scattering.

Ludlum Model 44-2 gamma scintillator

The Ludlum Model 44-2 gamma scintillator consists of a 2.54 × 2.54-cm NaI(Tl) crystal coupled to a photo-multiplier (PM) tube. The probe was connected to a Ludlum Model 16 Analyzer, which functioned as a counting rate meter. Measurements were performed with each source positioned along the axis of the detector at distances of 5 and 30 cm from the face of the probe. Background counts were recorded both before and after the source measurements.

Captus 3000 thyroid uptake system

The Captus 3000 thyroid uptake system incorporates a 5.08 × 5.08-cm NaI(Tl) crystal and PM tube detector assembly, and a 1,024-channel MCA. The detector assembly is located inside a lead-lined collimator.

Count rates were measured with each source positioned along the axis of the detector at two locations: near the end of the conical collimator (the actual location varied slightly for each source) and 50 cm from the aluminum housing that covers the NaI(Tl) crystal. An energy window, spanning a single region of interest, was set for each radio-nuclide. The energy windows and source-to-detector distances are listed in Table 2. Counts from ^{60}Co and ^{241}Am were measured using a single energy window for each radionuclide. Two sets of counts were measured from ^{137}Cs, using two distinct energy windows. All counts, including background, were accumulated for a period of 2 min.

TPM-903B portal monitor

The Model TPM-903B portal monitor was manufactured by TSA Systems Ltd. (now a part of Rapiscan Systems Inc.) and is distributed by Thermo Fisher Scientific Inc. (Franklin, MA, USA). As described by the manufacturer: “The system consists of twovertical pillars and an overhead cross-piece, which serves as an interconnect. The pillars are made of PVC [polyvinyl chloride] cell core pipe… The pillar spacing is fixed at 32” [81.28 cm] to provide adequate clearance for wheelchairs. Each pillar contains a radiation detector assembly and detector module. The system controller and occupancy detector are mounted on one of the vertical pillars.”‡‡

Fig. 1 shows a schematic diagram of the TPM-903B. Each radiation detector consists of a plastic scintillator in the form of a rectangular slab, 3.81 × 7.62 × 182.9 cm high, composed of polyvinyltoluene (PVT) with additional ingredients, and an acrylic light pipe and a PM tube that are coupled to the scintillator near the bottom of the pillar. The unit is equipped with lower and upper level discriminators (LLD and ULD) that can be adjusted by the user.

‡‡Thermo Fisher Scientific Inc. Transportable Portal Monitor Model TPM-903B: Operating and service manual, Doc. #5003 Rev. B (unpublished); 2010.

The demonstration unit used for these measurements had a space of 76.2 cm between the two pillars.

The LLD and ULD were first fixed at the assumed factory settings of 0.098 and 5.04 V.[§§] According to Thermo Fisher, "Approximately 1 volt of discriminator level equals 330 keV." These settings thus correspond to a nominal photon energy range of approximately 32.3–1,650 keV (TSA 2006). However, the system is reported to be very nonlinear at low energies, so that the actual low-energy threshold could be ±20 keV of the nominal value.[***]

To perform the measurements, the instrument was set to the background counting mode and the count time adjusted to 20 s, the maximum time that could be set on this monitor. The background count rate was measured first. The occupancy detector was then disabled so that the unit would always be in background mode. Such a procedure was necessary because, in the normal mode of operation, the monitor calculates a count rate using an integration time of 1 s. By counting in background mode, 20 times as many counts were accumulated, resulting in a more precise determination. Each of the three disk sources, in succession, was placed at the midpoint of the two pillars at the elevation of the calibration spots shown in Fig. 1. For the first set of measurements, the LLD was lowered to 0.054 V in order to achieve greater sensitivity, especially to the ^{241}Am source. The LLD was then restored to its assumed factory setting of 0.098 V, and the measurements were repeated.

Monte Carlo simulations of experimental measurements

Mathematical models of the instruments were constructed to perform Monte Carlo simulations of the radiation response of these instruments. These models were used to develop calibration factors that enable these instruments to be used to assess intakes of radionuclides by individuals with internal contamination. The models were validated by comparing the Monte Carlo simulations to the experimental results. The analysis also included a mathematical model of each radiation source and a model to simulate the transport of radiation from the source to the detector.

Radiation transport was modeled by means of MCNPX. The calculations used the MCNP pulse height tallies, which record detector events that fall into specified energy bins. The results are recorded as count per source photon and represent the probability that a photon emitted by the source would produce a pulse within the specified energy range.

An MCNP model of the Ludlum Model 44-2 gamma scintillator was constructed from engineering drawings furnished by Ludlum Measurements Inc., supplemented by telephone and email communications with Ludlum engineers. A cross-sectional view of the MCNP model that was generated by the MCNPX code package is shown in Fig. 2. Note that each material with the same density and composition is shown in a unique color.

A model of the Captus 3000 thyroid uptake probe was constructed from engineering drawings furnished by Capintec Inc., supplemented by telephone consultations and email

[§§]At the time of the experiment, there was conflicting information on whether the LLD factory setting was 0.068 or 0.098 V. Thermo Fisher Scientific Inc. later confirmed that 0.068 V is the standard for current instruments—it was 0.098 V on the older ones.
[***]Timothy Gregoire, Radiation Systems Engineer, Rapiscan Systems Inc., 21 November 2011, personal email to Robert Anigstein.

correspondence with Capintec engineers. A cross-sectional view of the model is shown in Fig. 3.

A model of the TPM-903B portal monitor was constructed from information provided by TSA (2006), Thermo Fisher,†† Eljen Technology (2010), and an official of TSA Systems Ltd.††† A cross section of the model of one column of the portal monitor is shown in Fig. 4. The plastic scintillators are offset from the centers of the PVC columns to allow room for the acrylic light pipes and PM tubes that are coupled to the scintillators near the bottom of each column.

The primary source of the decay schemes of radio-nuclides in the present study is the Evaluated Nuclear Structure Data File (ENSDF; BNL 2015). Data were also extracted from "ENDF/B-VII.1 Decay Data" (LANL 2012), which contains detailed listings of the ENSDF decay data in a readily accessible format, including detailed x-ray spectra not readily accessible from the Brookhaven National Laboratory website. Table 3 lists the photon spectra of the radionuclides used in the present analysis. Each spectrum encompasses more than 99.99% of the total intensity of photons with energies greater than 3.5 keV.

Gaussian energy distribution

Energy deposited in an NaI(Tl) crystal or a plastic scintillator produces a scintillation that in turn generates an electrical pulse in the detector system. The inherent statistics of the underlying processes produce a broadening of the photopeak. These processes cannot be explicitly modeled in standard Monte Carlo codes. However, a GEB treatment can be applied to the pulse height distribution to account for the energy resolution of the detector. Siciliano et al. (2008) also used GEB to represent the broadening of spectral lines from plastic scintillators due to nonstochastic effects such as the nonlinear relationship between light output and deposited energy and the dependence of light collection on position in a large detector.

MCNP uses the following expression to represent GEB:

$$F(E)=a+b\sqrt{E+cE^2}, \quad (1)$$

where

$F(E)$ = full width at half maximum (FWHM) (MeV);

E = energy deposited in detector (MeV); and

a, b, c = user-specified parameters.

When this feature is invoked by the user, GEB is applied to all events that deposit energy in the detector, most of which are from the Compton continuum rather than the photopeak.

†††Timothy Gregoire, Radiation Systems Engineer, Rapiscan Systems Inc., November 2011–October 2012, 12 personal emails to Robert Anigstein.

"The energy actually scored is sampled from a Gaussian with [the specified] FWHM" (Pelowitz 2011).

RESULTS

Ludlum Model 44-2 gamma scintillator

The normalized count rates derived from the measurements on the Ludlum Model 44-2 gamma scintillator are shown in Table 4. The measured count rates were corrected for dead-time losses, applying the following formula (Knoll 2010):

$$n = \frac{m}{1 - \mathrm{m}\tau}, \quad (2)$$

where

n = true count rate (cps);

m = observed count rate (cps); and

τ = dead time (s).

According to Ludlum Measurements Inc., the dead time for the Ludlum gamma scintillator coupled to a Ludlum Model 16 Analyzer is 10 μs.[‡‡‡]

An expression derived by Knoll (2010) for the standard deviation of measurements recorded on a counting rate meter, based on Poisson statistics, was used to calculate the standard deviations of the measured count rates:

$$\sigma_r = \sqrt{\frac{b + r}{2\tau}}, \quad (3)$$

where

σ_r = standard deviation of net count rate measured on a counting rate meter (s^{-1});

b = background count rate (s^{-1});

r = observed count rate (s^{-1}); and

τ = time constant of rate meter (s).

The time constant of the Model 16 Analyzer is not listed in the technical specifications of this instrument. However, Ludlum (2011) stated that the time from 10 to 90% of the final reading is 22 s with the *fast-slow* meter response switch in the *slow* position. The response time of the instrument can be expressed by the following equations, which were solved numerically to yield the time constant:

[‡‡‡]Ludlum Measurements Inc., 17 December 2015, personal email to Robert Anigstein.

$$1-e^{\frac{t_{10}}{\tau}}=0.1$$
$$1-e^{\frac{t_{90}}{\tau}}=0.9$$
$$t_{90}-t_{10}=t_{01\rightarrow 90},$$

where

τ = time constant (calculated); =10.6 s;

t_{10} = time to achieve 10% deflection (s);

t_{90} = time to achieve 90% deflection (s);

$t_{10\rightarrow 90}$ = time from 10 to 90% deflection; and = 22 s (Ludlum 2011).

The uncertainties in the experimental count rates listed in Table 4 are given by $\sigma_{r,x}=\sqrt{{\sigma_r}^2+x^2{c_v}^2}$. The relative uncertainties are in the range of 1.3–4.2%. These calculated uncertainties do not include the uncertainty in the analog meter on the Model 16 Analyzer. These uncertainties are listed for reference only—as discussed later, these values were not used in determining the overall goodness of fit between experimental and simulated results.

As an initial verification of the experimental data, the response of the instrument was simulated by using MCNPX to calculate the exposure rate in air from the ^{137}Cs source at a point corresponding to the center of the NaI(Tl) crystal. The “typical sensitivity” of 175 min^{-1} μR^{-1} h (4.07 × 10^{13} C kg^{-1}) cited by Ludlum (2014) was then used to calculate the count rate. The calculations yielded count rates of 1,636 and 101 s^{-1} for the two detector locations, while the measured net count rates were 1,635 and 100 s^{-1}, respectively. Given the uncertainties in the meter readings and in the calibration of the ^{137}Cs source, this constitutes excellent agreement and confirms the accuracy of the instrument calibration and of the laboratory measurements. This calculation did not use the MCNP model of this instrument.

To use the MCNPX results, which were tallied in 1-keV-wide bins starting at $E = 0$, to simulate the normalized experimental count rates, it was necessary to specify the low-energy threshold of the instrument. However, Ludlum could not provide the threshold energy for this detector. In order to determine the threshold energy that produced the best fit between the experimental measurements and the MCNPX simulations, the results of each of the MCNPX analyses for the various radio-nuclides and source locations were processed using a range of threshold energies down to 1 keV, the lower limit of the MCNPX energy range for photons and electrons.

The goodness of fit of the calculated to experimental data is based on the least root-mean-square (rms) weighted deviation of the data sets listed in Table 4. The weight assigned to each relative deviation is a function of the uncertainties of the calculated and the experimental data. As stated earlier, the standard deviation of the experimental results has two components: σ_r, derived from eqn (3), and c_V of the calibration sources, listed in Table 1. Since the same source was used for the measurements on a given radionuclide at two

source-to-detector distances, the experimental uncertainties listed in Table 4 were not applied to each individual measurement, since the source strength did not vary between measurements on that radionuclide. A two-step process was employed instead.

The first step was to determine the goodness of fit of the calculated to experimental data for each radionuclide by the following expression, which is partially based on Knoll (2010):

$$\overline{\Delta}_j = \sqrt{\frac{\sum_{i=1}^{n_j} \Delta_{i_j}^2 w_{i_j}}{\sum_{i=1}^{n_j} w_{i_j}}},$$

where

$\bar{\Delta}_j$ = rms relative deviation of calculated values for radioactive calibration source j from corresponding experimental measurements;

n_j = number of measurements on calibration source j;

Δ_{ij} = relative deviation of calculated value i for calibration source j from corresponding experimental measurement;

$$= \frac{y_{ij}}{x_{ij}} - 1$$

y_{ij} = count rate i derived from MCNPX simulation of calibration source j (s^{-1});

x_{ij} = net measured count rate i from calibration source j (s^{-1});

w_{ij} = weight assigned to Δ_{ij};

$$= \sigma_{\Delta_{ij}}^{-2}$$

$\sigma_{\Delta ij}$ = standard deviation of Δ_{ij};

$$= \sqrt{\frac{y_{ij}^2 \sigma_{r_{ij}}^2 + x_{ij}^2 \sigma_{y_{ij}}^2}{x_{ij}^2}}$$ (based on Knoll 2010); x^2

σ_{rij} = standard deviation of count rate i from calibration source j (s^{-1});

σ_{yij} = standard deviation of calculated MCNPX result i for calibration source j, derived from MCNPX output (s^{-1}).

Next, the goodness of fit of all the calculated to experimental data for a given instrument was determined by the following expression:

$$\bar{\Delta}' = \sqrt{\frac{\sum_{j=i}^{n_c} \bar{\Delta}_j^{\,2} w_j'}{\sum_{j=i}^{n_c} w_j'}}, \quad (4)$$

$\bar{\Delta}'$ = rms relative deviation of calculated values from corresponding experimental measurements on a given instrument;

n_c = number of calibration sources; and

w_j' = weight assigned to $\bar{\Delta}_j$

$$= \frac{1}{\frac{1}{n_j} + c_{v_j}^2}$$
$$\sum_{i=1} w_{ij}$$

cv_j = coefficient of variation of calibration source j.

The best agreement between the measured and calculated data was achieved by using a 1-keV threshold. Although this does not mean that the detector can in fact measure 1-keV photons, this threshold was used as a fitting parameter to match the measured data. The results of the comparison are shown in Table 4. The calculated count rates are based on MCNPX simulations that did not use GEB. The rms relative deviation $\bar{\Delta}'$ = 10.9%.

Captus 3000 thyroid uptake system

The experimental results for the Captus 3000 thyroid uptake system are listed in Table 2. The system incorporates dead time corrections into the count rate,[§§§] so no further corrections were required.

For instruments on which counts were accumulated for a fixed period of time, such as the Captus 3000 and the TPM-903B portal monitor, eqn (3) becomes

$$\sigma_c = \sqrt{\frac{b+r}{t_c}},$$

where σ_c = standard deviation of net count rate measured for a fixed time (s^{-1}), and t_c = counting time (equal times for background counts and source measurements) (s).

The measurements on ^{137}Cs employed both 10–750 keV and 108–686 keV windows. Although the narrower window produced lower background counts, it also lowered the counts from the source, resulting in higher relative errors.

[§§§]Mary Anne Yusko, Vice President, Product Development and Regulatory Affairs, 18 December 2015, personal email to Robert Anigstein.

The uncertainties in the experimental count rates, listed in Table 2, are given by $\sigma_x = \sqrt{\sigma_c{}^2 + x^2 c_v{}^2}$. The relative experimental uncertainties are in the range of 1.2–1.7%. These uncertainties are listed for reference only—the overall goodness of fit between experimental and simulated results was determined by eqn (4).

Since energy windows were set on this instrument during the experiment, the counts from the MCNPX simulations were summed over these energy ranges.**** The results of the comparison are shown in Table 2. The rms relative deviation $\bar{\Delta}' = 4.2\%$.

MCNPX simulations using a range of GEB parameters showed modest improvements in the fit to the measured data. However, since calculations that did not employ GEB showed acceptable agreement, this simpler model was adopted for this instrument.

TPM-903B portal monitor

The results of the experiments on the TPM-903B portal monitor are shown in Table 5. The measured count rates were corrected for dead-time losses using eqn (2). The dead time of the system was calculated to be 2.9 μs.††††

The uncertainties in the experimental count rates listed in Table 5 are given by $\sigma_x = \sqrt{\sigma_c{}^2 + x^2 c_v{}^2}$. The relative experimental uncertainties are in the range of 1.3–10.6%. The normalized count rates on the monitor were simulated using MCNPX, employing the GEB option. This approach is partly based on Siciliano et al. (2008), who used MCNP5 to simulate the response of a PVT scintillator in the shape of a right circular cylinder 5 cm thick and 36 cm in diameter to a point source of ^{137}Cs (the manufacturer of the detector was not identified). These authors, together with other investigators, reported that PVT plastic scintillators exhibit wide energy broadening. Full-energy photopeaks were not observed because the predominant interaction of high-energy photons was by Compton scattering. Siciliano et al. employed a one-parameter GEB function: a and c in eqn (1) in the present paper were set to zero. Adjusting b to yield widths equal to 1%, 14%, 25%, 50%, and 75% of the peak energy at 662 keV, they found that a value of 50% produced the best fit to the experimental spectrum. They explained that GEB was used “to lump together all the effects that generate the observed broad PVT spectra.”

In the present study, a series of MCNPX simulations were performed of the count rates on the portal monitor using a one-parameter GEB function. The parameter b was varied in discrete steps, centered on the value adopted by Siciliano et al. (2008). Because of the uncertainty of the low-energy threshold, the count rates for each value of the b parameter were calculated for a range of threshold energies, similar to the procedure used for the Ludlum gamma scintillator. The low-energy threshold that yielded the best agreement between the measured and simulated count rates (i.e., the lowest $\bar{\Delta}'$) was determined for each value of the b parameter and for each of the two LLD settings listed in Table 5. The best overall agreement was achieved by using a b parameter corresponding to an energy

****Energy calibration and constancy tests were performed on the instrument prior to the experimental measurements.
††††Timothy Gregoire, Radiation Systems Engineer, Rapiscan Systems Inc., 14 November 2011, personal email to Robert Anigstein.

resolution of 45% at 661.66 keV and threshold energies of 34.75 and 56 keV for the two LLD settings. The rms relative deviation $\bar{\Delta}' = 0.9\%$.

DISCUSSION

Ludlum Model 44-2 gamma scintillator

The results for the Ludlum Model 44-2 gamma scintillator listed in Table 4 show that the Δs are negative, with the calculated values differing by −5.2 to −15.8% from the experimental values, which indicates that the MCNPX calculations consistently underestimate the count rates. Underpredicting the count rates would lead to a more conservative assessment if the model were used to estimate the intakes of radionuclides and subsequent doses to individuals with internal contamination.

Captus 3000 thyroid uptake system

The results for the Captus 3000 thyroid uptake system listed in Table 2 show acceptable agreement between the calculated and measured count rates, with differences ranging from −9 to +6%. The count rate from the ^{137}Cs source at 17.25 cm from the detector, using the 10–750 keV energy window, appears to be an outlier. However, since there is no sound basis for discarding this measurement, it was retained in the analysis.

TPM-903B portal monitor

The results for the TPM-903B portal monitor listed in Table 5 show excellent agreement between the calculated and experimental count rates. The differences in the six sets of count rates range from −4.9 to +1.1%. It should be noted that the uncertainty of each difference, listed as an absolute percentage in the far right column, exceeds the absolute value of the difference. Therefore, the measured and calculated values agree within the combined experimental and statistical errors.

The energy resolution of the TPM-903B is affected by the nonlinearity of this system at low energies and by the dependence of the signal on the spatial position of the incident photon in the 183-cm-long detectors, as well as by the stochastic nature of the scintillation process. The GEB function accounts for the combined effect of these physical phenomena. The GEB parameter and the corresponding low-level energy thresholds derived in the present study should be viewed as fitting parameters in a model that can allow this instrument to be used in the assessment of intakes of radio-nuclides by an affected individual.

CONCLUSION

The present study validated the MCNP models of three instruments: the Ludlum Model 44-2 gamma scintillator, the Captus 3000 thyroid uptake system, and the TPM-903B portal monitor. In all three cases, agreement between the measured and calculated values was achieved without the use of empirical radionuclide-dependent scaling factors that were employed by other investigators. The utility of these instruments for the in vivo assessments of affected individuals will be evaluated in a forthcoming publication that will describe the

computer simulations of the response of these instruments to radionuclides distributed in various anatomical regions of the human body as a function of time and mode of intake.

Acknowledgments

The authors gratefully acknowledge the support and assistance of the following individuals and organizations. The Penn State Milton S. Hershey Medical Center provided access to its facilities. Richard Olsher, HP Consulting LLC, provided support for the MCNPX simulations and reviewed an earlier version of the present paper. Michael Mallett reviewed a draft of the present paper. Harry Chmelynski, Senior Statistician, S. Cohen & Associates, reviewed the methodology used in the statistical analysis of count rate measurements. Ludlum Measurements Inc. provided engineering drawings and detailed technical information on the Ludlum Model 44-2 gamma scintillator and furnished an instrument for use in the study. Mary Anne Yusko, Vice President, Product Development and Regulatory Affairs, Capintec Inc., furnished engineering drawings and other technical information on the Captus 3000 thyroid uptake system and provided a unit for the study. Timothy Gregoire, Radiation Systems Engineer, Rapiscan Systems Inc., provided detailed technical information on the Model TPM-903B portal monitor. Richard P. Oxford, Commercial Manager; Handhelds, Transportables and Applications, Thermo Fisher Scientific Inc., provided technical support for this instrument and a demonstration unit for the experiments.

This work was supported by Contract No. GS-10F-0093K from the Centers for Disease Control and Prevention (CDC) with S. Cohen & Associates (SC&A Inc.) Additional support was provided by SciMetrika LLC, under Contract No. 200-2009-28540, Task Order 0008. The contents are solely the responsibility of the authors and do not necessarily represent the official views of the CDC.

References

Anigstein, R., Engdahl, JC., Erdman, MC., King, SH., Mauro, JJ., Miller, KL., Olsher, RH. [Accessed 8 May 2015] Use of radiation detection, measuring, and imaging instruments to assess internal contamination from intakes of radionuclides. Parts I–V [online]. 2007–2010. Available at www.bt.cdc.gov/radiation/clinicians/evaluation/supportdocs.htm

Argonne National Laboratory, Environmental Science Division. [Accessed 9 May 2015] Human health fact sheet, August 2005: radiological dispersal device (RDD); Radiological and chemical fact sheets to support health risk analyses for contaminated areas [online]. 2007. p. 80-85.[unnumbered pp. in PDF file]. Available at www.remm.nlm.gov/ANL_ContaminantFactSheets_All_070418.pdf

Brookhaven National Laboratory, National Nuclear Data Center. [Accessed 16 June 2015] Evaluated nuclear structure data file (ENSDF) [online]. 2015. Available at www.nndc.bnl.gov/ensdf/

Dewji S, Hertel N, Ansari A. Assessing internal contamination after the detonation of a radiological dispersion device using a 2 × 2-inch sodium iodide detector. Radiat Protect Dosim. 2013; 155:300–316.

Eljen Technology. [Accessed 7 May 2015] EJ-200 plastic scintillator. Data sheet [online]. 2010. Available at www.eljentechnology.com/index.php?option=com_content&view=article&id=48:ej-200&catid=31&Itemid=46

Knoll, GF. Radiation detection and measurement. 4. New York: John Wiley & Sons Inc; 2010.

Kramer GH, Capello K, Hauck BM. The HML's new field deployable, high-resolution whole body counter. Health Phys. 2005; 89(Supplement 5):S60–S68. [PubMed: 16224263]

Los Alamos National Laboratory. MCNP5/MCNPX: Monte Carlo N-Particle transport code system including MCNP5-1. 60 and MCNPX 2.7.0 and data libraries, RSICC Code Package CCC-740 [computer software and manual]. Oak Ridge, TN: Oak Ridge National Laboratory; 2011. (CD-ROM)

Los Alamos National Laboratory. [Accessed 9 May 2015] ENDF/B-VII.1 decay data [online]. 2012. Available at http://t2.lanl.gov/nis/data/endf/decayVII.1.html

Ludlum Measurements, Inc. [Accessed 9 May 2015] Ludlum Model 16 analyzer [online]. 2011. Available at http://ludlums.com/images/stories/product_manuals/M16.pdf

Ludlum Measurements, Inc. [Accessed 9 May 2015] Ludlum Model 44-2 gamma scintillator [online]. 2014. Available at http://ludlums.com/images/stories/product_manuals/M44-2.pdf

Manger RP, Hertel NE, Burgett EA, Ansari A. Using handheld plastic scintillator detectors to triage individuals exposed to a radiological dispersal device. Radiat Protect Dosim. 2012; 150:101–108.

National Council on Radiation Protection and Measurements. Management of persons contaminated with radionuclides: handbook. Bethesda, MD: 2008. NCRP Report No. 161

Pelowitz, DB. MCNPX user's manual version 2.7.0, LA-CP-11-00438. Los Alamos National Laboratory. MCNP5/MCNPX: Monte Carlo N-Particle transport code system including MCNP5-1.60 and MCNPX 2.7.0 and data libraries, RSICC Code Package CCC-740 [computer software and manual]. Oak Ridge National Laboratory; Oak Ridge, TN: 2011. (CD-ROM)

Scarboro S, Hertel N, Burgett E, Howell R, Ansari A. Validation of Monte Carlo simulation of a thyroid uptake system using various sources and a slab phantom. Nucl Technol. 2009; 168:169–172.

Siciliano ER, Ely JH, Kouzes RT, Schweppe JE, Strachan DM, Yokuda ST. Energy calibration of gamma spectra in plastic scintillators using Compton kinematics. Nucl Instrum Methods Phys Res A. 2008; 594:232–243.

TSA Systems, Ltd. Transportable Portal Monitor Model TPM-903B: operating and service manual, Doc. #5003 Rev. A [online]. 2006. Available at www.laurussystems.com/Service/TPM-903B_User-Guide_092009.pdf

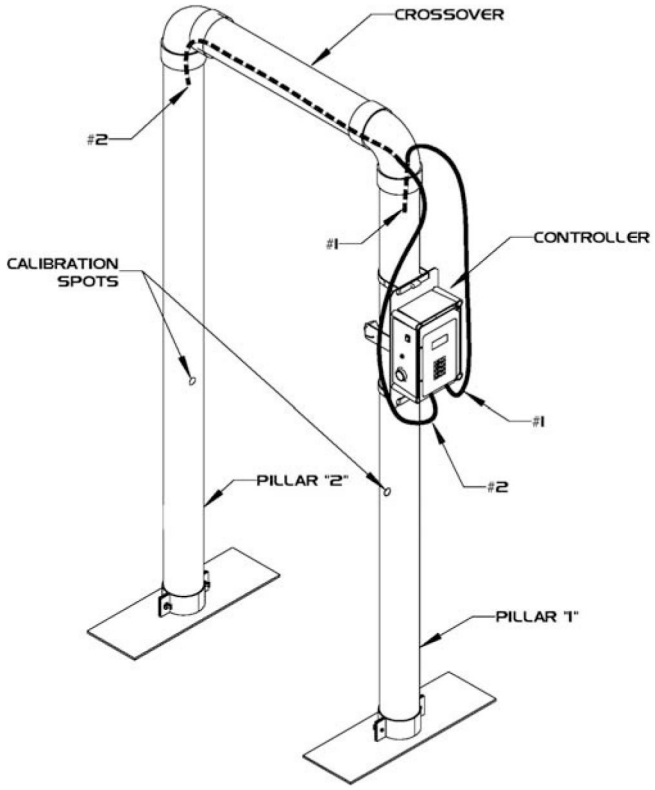

Fig. 1.
Schematic Diagram of TPM-903B Portal Monitor (TSA 2006).

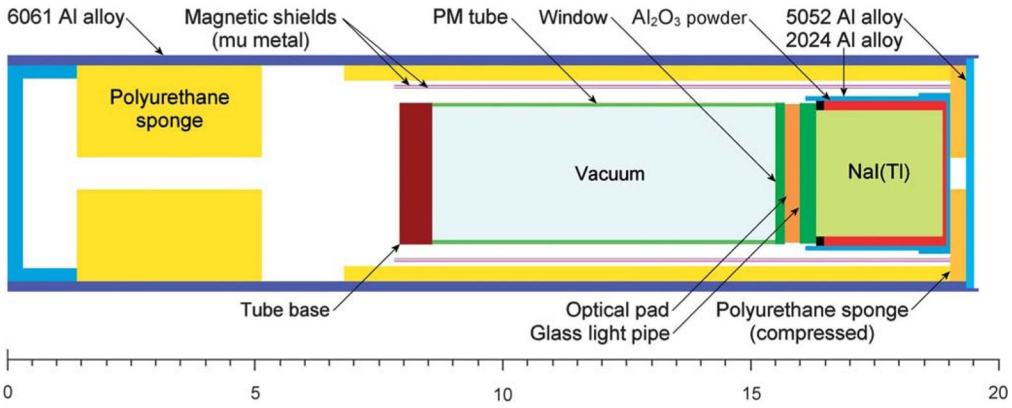

Fig. 2.
MCNP model of Ludlum 44-2 gamma scintillator (scale in cm).

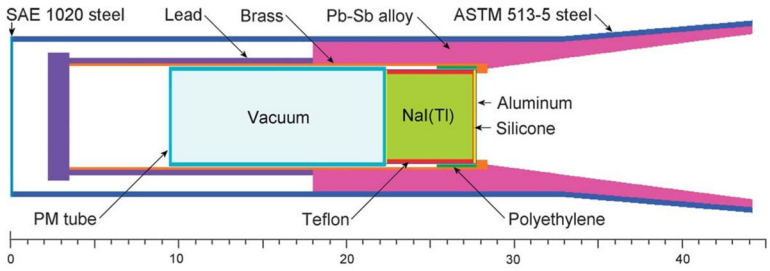

Fig. 3.
MCNP model of Captus 3000 thyroid probe (scale in cm).

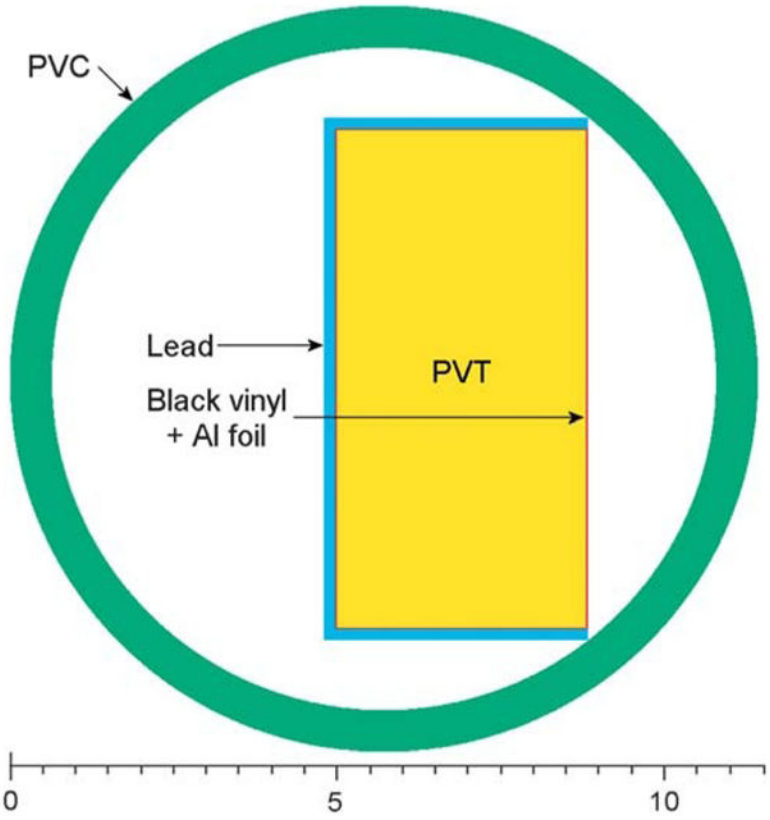

Fig. 4.
MCNP model of TPM-903B portal monitor (scale in cm).

Table 1

Radioactive calibration sources.

			Uncertainty (%)	
Radionuclide	**Half-life[a] (y)**	**Activity (kBq)**	**99th %ile[b]**	**c_v**
^{60}Co	5.2712	140	3.1	1.20
^{137}Cs	30.08	303	3.1	1.20
^{241}Am	432.6	331	3.44	1.33

[a] BNL (2015).

[b] Certified by manufacturer.

Table 2

Comparison of experimental and calculated count rates on Captus 3000 Thyroid Uptake System.

			Experiment (s^{-1} Bq^{-1})		MCNPX (s^{-1} Bq^{-1})		Comparison	
Nuclide	**Energy window (keV)**	**Distance (cm)**	x	σ_x	y	σ_y [a]	Δ_b	σ_Δ [c]
^{60}Co	10–1,400	17.7	7.53×10^{-3}	9.30×10^{-5}	7.53×10^{-3}	4.90×10^{-6}	0.0%	1.2%
		50.0	9.67×10^{-4}	1.43×10^{-5}	9.64×10^{-4}	6.27×10^{-7}	−0.2%	1.5%
^{137}Cs	10–750	17.25	4.26×10^{-3}	5.24×10^{-5}	3.87×10^{-3}	7.16×10^{-6}	−9.0%	1.2%
		50.0	5.05×10^{-4}	7.26×10^{-6}	4.95×10^{-4}	1.02×10^{-6}	−1.9%	1.4%
	108–686	17.25	3.25×10^{-3}	4.02×10^{-5}	3.17×10^{-3}	6.55×10^{-6}	−2.4%	1.3%
		50.0	3.98×10^{-4}	5.94×10^{-6}	4.10×10^{-4}	9.37×10^{-7}	3.1%	1.5%
^{241}Am	10–72	17.35	2.36×10^{-3}	3.24×10^{-5}	2.38×10^{-3}	1.87×10^{-6}	0.9%	1.4%
		50.0	2.76×10^{-4}	4.56×10^{-6}	2.93×10^{-4}	5.05×10^{-7}	6.0%	1.7%

[a] Calculated from MCNPX results.

[b] MCNPX ÷ exp − 1.

[c] Standard deviation of Δ.

Table 3

Photon spectra of radionuclides used in present analysis.[a]

^{60}Co		^{137}Cs		^{241}Am	
E (keV)	**I (%)**	**E (keV)**	**I[b] (%)**	**E (keV)**	**I (%)**
7.41782	0.0032	4.47	0.9147	13.5114	1.5489
7.43578	0.0062	31.817	1.9928	13.9387	10.7295
8.22231	0.0004	32.194	3.6352	17.5392	10.543
8.22459	0.0008	36.304	0.3479	21.1288	2.4119
347.14	0.0075	36.378	0.6718	26.3446	2.27
826.1	0.0076	37.255	0.2125	33.196	0.126
1,173.22	99.85	661.657	85.1	42.704	0.0055
1,332.49	99.9826	Total	92.875	43.42	0.073
2,158.57	0.0012			55.56	0.0181
Total	199.8595			59.5409	35.9
				69.76	0.0029
				97.498	0.0011
				98.97	0.0203
				101.574	0.0018
				102.98	0.0195
				125.3	0.0041
				Total	63.6756

[a] Adapted from BNL (2015) and LANL (2012). Values used in MCNPX analyses, except as noted. Listed precision may exceed precision of adopted values.

[b] Values rounded.

Table 4

Comparison of experimental and calculated count rates on Ludlum Model 44–2 gamma scintillator.

		Experiment (s^{-1} Bq^{-1})		MCNPX (s^{-1} Bq^{-1})		Comparison	
Nuclide	**Distance (cm)**	x	$\sigma_{r,x}$	y	σ_y [a]	Δ [b]	σ_Δ [c]
^{60}Co	5	8.25×10^{-3}	1.13×10^{-4}	7.82×10^{-3}	5.48×10^{-6}	−5.2%	1.4%
	30	4.04×10^{-4}	1.69×10^{-5}	3.61×10^{-4}	1.44×10^{-6}	−10.7%	3.8%
^{137}Cs	5	5.40×10^{-3}	7.13×10^{-5}	4.86×10^{-3}	2.92×10^{-6}	−9.9%	1.3%
	30	2.48×10^{-4}	8.55×10^{-6}	2.19×10^{-4}	7.01×10^{-7}	−11.6%	3.1%
^{241}Am	5	5.15×10^{-3}	7.41×10^{-5}	4.34×10^{-3}	2.17×10^{-6}	−15.8%	1.3%
	30	1.74×10^{-4}	7.13×10^{-6}	1.58×10^{-4}	4.73×10^{-7}	−9.5%	3.7%

[a] Calculated from MCNPX results.

[b] MCNPX ÷ exp − 1.

[c] Standard deviation of Δ.

Table 5

Comparison of experimental and calculated count rates on TPM-903B portal monitor.

			Experiment (s^{-1} Bq^{-1})		MCNPX (s^{-1} Bq^{-1})		Comparison	
Nuclide	**Electronic LLD (V)**	**Threshold energy (keV)**	**Count rate**	**σ_e**	**Count rate**	**σ_y [a]**	**Δ [b]**	**σ_Δ [c]**
^{60}Co	0.054	34.8	2.97×10^{-2}	3.87×10^{-4}	2.94×10^{-2}	2.94×10^{-5}	−1.1%	1.3%
	0.098	56.0	2.84×10^{-2}	3.70×10^{-4}	2.83×10^{-2}	2.83×10^{-5}	−0.4%	1.3%
^{137}Cs	0.054	34.8	1.47×10^{-2}	1.90×10^{-4}	1.47×10^{-2}	1.32×10^{-5}	−0.2%	1.3%
	0.098	56.0	1.36×10^{-2}	1.76×10^{-4}	1.37×10^{-2}	1.37×10^{-5}	1.1%	1.3%
^{241}Am	0.054	34.8	9.07×10^{-4}	4.86×10^{-5}	9.14×10^{-4}	3.56×10^{-6}	0.8%	5.4%
	0.098	56.0	4.03×10^{-4}	4.26×10^{-5}	3.83×10^{-4}	2.34×10^{-6}	−4.9%	10.1%

[a] Calculated from MCNPX results.

[b] MCNPX ÷ exp − 1.

[c] Standard deviation of Δ.